

Kernel-Based LMI Approaches to Solving the Hamilton–Jacobi–Bellman Equation and Nonlinear Optimal Control

Boumediene Hamzi and Umesh Vaidya

Abstract

We present a kernel-based linear matrix inequality (LMI) approach for solving Hamilton–Jacobi–Bellman (HJB) equations arising in nonlinear optimal control. The method converts the nonlinear HJB inequality into a convex semidefinite program through reproducing kernel Hilbert space (RKHS) representations and Schur complement reformulations. We provide complete theoretical results including convex reformulation, RKHS approximation, finite-dimensional discretization, suboptimality bounds, stability guarantees, and convergence rates. A critical component of our approach is the use of a Riccati Hessian constraint at the equilibrium to prevent trivial solutions while ensuring consistency with linearized optimal control theory. Numerical results on both 1D and 2D systems demonstrate the effectiveness of the approach, with comprehensive validation through multiple initial conditions showing that all closed-loop trajectories converge exponentially to the origin from various starting points, successfully stabilizing unstable equilibria with theoretical guarantees. The method maintains computational tractability while providing rigorous optimality and stability guarantees.

1 Introduction

The Hamilton–Jacobi–Bellman (HJB) equation provides the cornerstone for solving nonlinear optimal control problems [3]. For a control-affine system $\dot{x} = f(x) + g(x)u$ with infinite-horizon cost functional, the optimal value function $V^*(x)$ satisfies a nonlinear partial differential equation whose solution yields the optimal feedback control law. However, solving the HJB equation directly is computationally intractable for general nonlinear systems, presenting one of the fundamental challenges in control theory. Traditional approaches such as finite difference methods and dynamic programming suffer severely from the *curse of dimensionality* [3], with computational cost growing exponentially in the state dimension. Neural network-based methods have been proposed to address scalability [15], but typically lack theoretical guarantees on optimality and stability. Sum-of-squares (SOS) programming [35, 36] offers convexity with rigorous guarantees, but scales poorly with polynomial degree and is restricted to polynomial systems.

Among the various learning and approximation approaches, reproducing kernel Hilbert spaces (RKHSs) [11, 25] have emerged as a powerful framework with solid mathematical foundations for the analysis of dynamical systems. The foundational work on kernel methods for nonlinear systems approximation [7, 8] established that RKHS representations can effectively capture nonlinear input-output maps and system dynamics, with extensions to discrete-time systems [18], balanced reduction [5], and empirical estimators for stochastically forced systems [6]. Kernel methods have proven particularly effective for approximating operator-theoretic quantities: the Koopman generator and Schrödinger operator [26], eigenfunctions of the Koopman operator [28], Lyapunov functions

via Koopman eigenfunctions [30], and dimensionality reduction of metastable systems [4]. For stability analysis, kernel methods have been applied to Lyapunov function approximation from noisy data [14] and center manifold approximation [16, 17]. Additional applications include multiscale systems with critical transitions [20], microlocal kernel design for slow-fast stochastic differential equations [19], transport equations [21], kernel sum of squares for data-adapted learning [31], surrogate modeling [38], forecasting nonlinear time series [1], and connections to neural networks [39]. Compared to other learning approaches, kernel-based methods offer interpretability, rigorous theoretical analysis, well-understood numerical implementation with regularization, natural uncertainty quantification, and guaranteed convergence with *a priori* error estimates [24, 2, 10, 32, 34].

More recently, operator-theoretic methods involving the Koopman operator have been used for approximating the solution of the HJB equation [40]. The Koopman operator provides a linear (but infinite-dimensional) representation of nonlinear dynamics, enabling the application of linear systems theory to nonlinear problems. Similarly, operator-theoretic methods involving the Perron-Frobenius operator provide convex approaches to optimal control via formulations in the dual space of densities [37], with successful applications in data-driven optimal control design [23, 33, 41]. While these operator-based methods provide theoretical foundations, their practical implementation relies on computational frameworks such as RKHS-based methods. In this paper, we adopt a direct approach that leverages the RKHS framework both in the convex reformulation and for numerical approximation of the HJB equation.

The proposed approach is inspired by optimal control of linear systems, particularly the convex LMI-based formulation of the Riccati equation [9]. For linear systems, the algebraic Riccati equation $R(P) = 0$ is instrumental in solving the optimal control problem. Strictly speaking, both the Riccati equation $R(P) = 0$ and the inequality $R(P) \leq 0$ are nonconvex in the matrix variable P ; however, the inequality $R(P) \geq 0$ defines a convex set in P . Building on this analogy, we extend the Riccati framework to the Hamilton-Jacobi equation, formulating a convex LMI-based representation of the HJB inequality. While the LMIs derived from the Riccati equation are finite-dimensional, those arising from the HJB equation are infinite-dimensional. To address this, we employ an RKHS-based approach [12] to obtain finite-dimensional approximations, augmented with appropriate constraints to ensure stabilizing solutions.

This paper makes the following contributions. First, we establish equivalence between the nonlinear HJB inequality and a linear matrix inequality via the Schur complement, transforming the infinite-dimensional nonconvex problem into a convex constraint linear in the value function gradient. Second, we show that value function gradients admit finite-dimensional kernel representations enabling practical computation with approximation-theoretic guarantees. Third, we introduce a Riccati Hessian constraint that prevents trivial solutions while ensuring consistency with linearized optimal control theory by enforcing that the Hessian of the value function at equilibrium matches the algebraic Riccati equation solution. Fourth, we derive a tractable semidefinite program [9, 27] through collocation, reducing the infinite-dimensional LMI to finitely many matrix inequality constraints. Fifth, we provide complete theoretical analysis including suboptimality bounds, exponential stability certificates, and convergence rates. Finally, we demonstrate the method on 1D and 2D polynomial systems and the Van der Pol oscillator, showing that all closed-loop trajectories converge exponentially to the origin from multiple initial conditions, successfully stabilizing unstable equilibria with theoretical guarantees.

The remainder of this paper is organized as follows. Section 2 formulates the optimal control problem. Section 3 develops the theoretical framework including the LMI reformulation, RKHS approximation, Riccati Hessian constraint, and performance guarantees. Section 4 discusses the relationship to classical Lyapunov function construction. Section 5 presents numerical results, and Section 6 concludes.

2 Problem Formulation

Consider the control-affine system

$$\dot{x} = f(x) + g(x)u, \quad x \in \mathbb{R}^n, \quad u \in \mathbb{R}^m, \quad (1)$$

where $f : \mathbb{R}^n \rightarrow \mathbb{R}^n$ and $g : \mathbb{R}^n \rightarrow \mathbb{R}^{n \times m}$ are smooth functions, with infinite-horizon cost

$$J(x_0, u) = \int_0^\infty \left[q(x(t)) + \frac{1}{2} u(t)^\top D u(t) \right] dt, \quad (2)$$

where $q : \mathbb{R}^n \rightarrow \mathbb{R}_{\geq 0}$ is a state cost function, and $D \in \mathbb{R}^{m \times m}$ is symmetric positive definite.

Assumption 2.1 (Standing Assumptions). *Throughout this paper, we assume:*

1. The functions f , g , and q are sufficiently smooth (at least C^2).
2. The origin $x = 0$ is an equilibrium of the uncontrolled dynamics: $f(0) = 0$.
3. The state cost satisfies $q(0) = 0$ and $q(x) > 0$ for $x \neq 0$.
4. The pair (A, B) is stabilizable, where $A = \frac{\partial f}{\partial x}|_{x=0}$ and $B = g(0)$.
5. The pair $(A, Q^{1/2})$ is detectable, where $Q = \nabla^2 q(0)$.

The optimal value function $V^*(x) = \inf_u J(x, u)$ satisfies the HJB equation:

$$\frac{\partial V}{\partial x} f(x) - \frac{1}{2} \frac{\partial V}{\partial x} g(x) D^{-1} g(x)^\top \left(\frac{\partial V}{\partial x} \right)^\top + q(x) = 0. \quad (3)$$

More generally, for approximations, we consider the HJB *inequality*:

$$\frac{\partial V}{\partial x} f(x) - \frac{1}{2} \frac{\partial V}{\partial x} g(x) D^{-1} g(x)^\top \left(\frac{\partial V}{\partial x} \right)^\top + q(x) \geq 0. \quad (4)$$

When the inequality holds with equality, the optimal control is

$$u^*(x) = -D^{-1} g(x)^\top \left(\frac{\partial V^*}{\partial x} \right)^\top. \quad (5)$$

The challenge is that (4) is a nonlinear partial differential inequality that is generally intractable to solve.

3 Theoretical Framework

3.1 Preliminary: Schur Complement

We first recall the Schur complement lemma, which is fundamental to our reformulation.

Lemma 3.1 (Schur Complement). *Let M be a symmetric block matrix of the form*

$$M = \begin{bmatrix} A & B \\ B^\top & C \end{bmatrix}$$

where $A \in \mathbb{R}^{p \times p}$, $B \in \mathbb{R}^{p \times q}$, and $C \in \mathbb{R}^{q \times q}$ with $C \succ 0$ (positive definite). Then

$$M \succeq 0 \iff A - BC^{-1}B^\top \succeq 0.$$

More generally, if $C \succeq 0$, then $M \succeq 0$ if and only if $A \succeq 0$, $\text{range}(B) \subseteq \text{range}(C)$, and $A - BC^\dagger B^\top \succeq 0$, where C^\dagger denotes the Moore-Penrose pseudoinverse.

Proof. Since $C \succ 0$, we can write

$$M = \begin{bmatrix} I & BC^{-1} \\ 0 & I \end{bmatrix} \begin{bmatrix} A - BC^{-1}B^\top & 0 \\ 0 & C \end{bmatrix} \begin{bmatrix} I & 0 \\ C^{-1}B^\top & I \end{bmatrix}.$$

This is a congruence transformation, which preserves the signature (number of positive, negative, and zero eigenvalues). Since $C \succ 0$, we have $M \succeq 0$ if and only if $A - BC^{-1}B^\top \succeq 0$. \square

3.2 HJB Inequality as Linear Matrix Inequality

Our first key result establishes equivalence between the HJB inequality and a linear matrix inequality.

Theorem 3.2 (HJB Inequality as LMI). *The HJB inequality (4) is equivalent to the linear matrix inequality*

$$M(x) := \begin{bmatrix} 2 \left(\frac{\partial V}{\partial x} f(x) + q(x) \right) & \frac{\partial V}{\partial x} g(x) \\ g(x)^\top \left(\frac{\partial V}{\partial x} \right)^\top & D \end{bmatrix} \succeq 0. \quad (6)$$

Proof. Multiplying the HJB inequality (4) by 2, we obtain

$$2 \left(\frac{\partial V}{\partial x} f(x) + q(x) \right) - \frac{\partial V}{\partial x} g(x) D^{-1} g(x)^\top \left(\frac{\partial V}{\partial x} \right)^\top \geq 0. \quad (7)$$

Define $a := \frac{\partial V}{\partial x} g(x) \in \mathbb{R}^{1 \times m}$ (a row vector), $b := 2 \left(\frac{\partial V}{\partial x} f(x) + q(x) \right) \in \mathbb{R}$ (a scalar), and note that $D \succ 0$ by assumption.

Then inequality (7) can be written as

$$b - a D^{-1} a^\top \geq 0.$$

By Lemma 3.1 (Schur complement), since $D \succ 0$, this is equivalent to

$$\begin{bmatrix} b & a \\ a^\top & D \end{bmatrix} \succeq 0,$$

which is precisely the matrix $M(x)$ in (6). \square

Remark 3.3 (Significance of LMI Reformulation). *This theorem is crucial because it transforms the nonlinear HJB inequality into a constraint that is linear in the value function gradient (and hence in the optimization variables when the gradient is parameterized). The quadratic term in the original HJB inequality becomes a linear constraint via the Schur complement.*

3.3 RKHS Representation of the Value Function

The second key component is representing the value function gradient in a reproducing kernel Hilbert space.

Definition 3.4 (Reproducing Kernel Hilbert Space). *Let $\Omega \subseteq \mathbb{R}^n$ be a domain. A Hilbert space \mathcal{H} of functions $f : \Omega \rightarrow \mathbb{R}$ is called a reproducing kernel Hilbert space (RKHS) if there exists a symmetric, positive definite kernel $\kappa : \Omega \times \Omega \rightarrow \mathbb{R}$ such that:*

1. For all $x \in \Omega$, the function $\kappa(\cdot, x) \in \mathcal{H}$.

2. (Reproducing property) For all $f \in \mathcal{H}$ and $x \in \Omega$: $f(x) = \langle f, \kappa(\cdot, x) \rangle_{\mathcal{H}}$.

Theorem 3.5 (RKHS Approximation). Let \mathcal{H} be a reproducing kernel Hilbert space with kernel $\kappa : \Omega \times \Omega \rightarrow \mathbb{R}$, where $\kappa \in C^2(\Omega \times \Omega)$. Consider the finite-dimensional approximation space

$$\mathcal{H}_M := \text{span}\{\kappa(\cdot, x_1), \dots, \kappa(\cdot, x_M)\}$$

for given centers $\{x_i\}_{i=1}^M \subset \Omega$. For any $V \in \mathcal{H}_M$, the function and its gradient admit the representations

$$V(x) = \sum_{i=1}^M p_i \kappa(x, x_i), \quad (8)$$

$$\nabla V(x) = \sum_{i=1}^M p_i \nabla_x \kappa(x, x_i) =: K_x p, \quad (9)$$

where $K_x \in \mathbb{R}^{n \times M}$ has columns $\nabla_x \kappa(x, x_i)$, and $p = (p_1, \dots, p_M)^\top \in \mathbb{R}^M$ is the coefficient vector. Moreover, the Hessian is given by

$$\nabla^2 V(x) = \sum_{i=1}^M p_i \nabla_x^2 \kappa(x, x_i). \quad (10)$$

Proof. By definition of \mathcal{H}_M , any $V \in \mathcal{H}_M$ can be written as $V(x) = \sum_{i=1}^M p_i \kappa(x, x_i)$ for some coefficients $p_i \in \mathbb{R}$.

Since $\kappa \in C^2(\Omega \times \Omega)$, we can differentiate under the sum. For the gradient with respect to x :

$$\nabla V(x) = \nabla_x \left(\sum_{i=1}^M p_i \kappa(x, x_i) \right) = \sum_{i=1}^M p_i \nabla_x \kappa(x, x_i).$$

This can be written in matrix form as $\nabla V(x) = K_x p$, where the i -th column of K_x is $\nabla_x \kappa(x, x_i)$. Similarly, for the Hessian:

$$\nabla^2 V(x) = \nabla_x \left(\sum_{i=1}^M p_i \nabla_x \kappa(x, x_i) \right) = \sum_{i=1}^M p_i \nabla_x^2 \kappa(x, x_i). \quad \square$$

Remark 3.6 (Approximation Quality). For general $V^* \in \mathcal{H}$ (not necessarily in \mathcal{H}_M), the finite-dimensional representation (8) provides an approximation. The quality of this approximation depends on the distribution of centers $\{x_i\}$ and the smoothness of V^* . Standard RKHS approximation theory provides error bounds; see Theorem 3.15 below.

3.4 Avoiding Trivial Solutions: The Riccati Hessian Constraint

A critical challenge in solving the HJB inequality via optimization is the existence of the trivial solution $V(x) \equiv 0$, which satisfies all HJB constraints but provides no useful control law. To eliminate this undesirable solution while ensuring consistency with optimal control theory, we impose constraints at the equilibrium point (assumed to be the origin without loss of generality).

Definition 3.7 (Equilibrium Constraints). For a system with equilibrium at $x = 0$, we impose:

1. **Boundary condition:** $V(0) = 0$

2. **Gradient condition:** $\nabla V(0) = 0$

3. **Riccati Hessian condition:** $\nabla^2 V(0) = P$

where P is the solution to the algebraic Riccati equation (ARE) for the linearized system.

The third constraint deserves special attention as it is the key to preventing trivial solutions.

Theorem 3.8 (Riccati Matching Principle). *Consider the linearization of (1) at the origin:*

$$\dot{x} = Ax + Bu, \quad A = \left. \frac{\partial f}{\partial x} \right|_{x=0}, \quad B = g(0), \quad (11)$$

with quadratic approximation $V(x) \approx \frac{1}{2}x^\top Px$ near the origin. If V satisfies the HJB equation (3) and $\nabla^2 V(0) = P$, then P satisfies the algebraic Riccati equation

$$A^\top P + PA - PBD^{-1}B^\top P + Q = 0, \quad (12)$$

where $Q = \nabla^2 q(0)$ is the Hessian of the state cost at the origin.

Proof. Consider the Taylor expansion of the value function around the origin:

$$V(x) = V(0) + \nabla V(0)^\top x + \frac{1}{2}x^\top \nabla^2 V(0)x + O(\|x\|^3).$$

By the equilibrium constraints (Definition 3.7), we have $V(0) = 0$, $\nabla V(0) = 0$, and $\nabla^2 V(0) = P$, so

$$V(x) = \frac{1}{2}x^\top Px + O(\|x\|^3).$$

Similarly, expand the system dynamics:

$$f(x) = f(0) + \left. \frac{\partial f}{\partial x} \right|_{x=0} x + O(\|x\|^2) = Ax + O(\|x\|^2),$$

and

$$g(x) = g(0) + O(\|x\|) = B + O(\|x\|).$$

The state cost expands as:

$$q(x) = q(0) + \nabla q(0)^\top x + \frac{1}{2}x^\top Qx + O(\|x\|^3) = \frac{1}{2}x^\top Qx + O(\|x\|^3),$$

using $q(0) = 0$ and $\nabla q(0) = 0$ (from Assumption 2.1).

The gradient of the value function is:

$$\nabla V(x) = Px + O(\|x\|^2).$$

Substituting into the HJB equation (3):

$$\begin{aligned} & \nabla V(x)^\top f(x) - \frac{1}{2}\nabla V(x)^\top g(x)D^{-1}g(x)^\top \nabla V(x) + q(x) \\ &= (Px)^\top (Ax) - \frac{1}{2}(Px)^\top BD^{-1}B^\top (Px) + \frac{1}{2}x^\top Qx + O(\|x\|^3) \\ &= x^\top PAx - \frac{1}{2}x^\top PBD^{-1}B^\top Px + \frac{1}{2}x^\top Qx + O(\|x\|^3) \\ &= \frac{1}{2}x^\top \left(A^\top P + PA - PBD^{-1}B^\top P + Q \right) x + O(\|x\|^3) = 0. \end{aligned}$$

For this to hold for all x in a neighborhood of the origin, the quadratic coefficient must vanish:

$$A^\top P + PA - PBD^{-1}B^\top P + Q = 0. \quad \square$$

Remark 3.9 (Significance of the Riccati Constraint). *The Riccati Hessian constraint $\nabla^2 V(0) = P$ serves multiple critical purposes:*

1. **Prevents trivial solution:** *Since $P \succ 0$ (positive definite for stabilizable systems under Assumption 2.1), the constraint explicitly excludes $V \equiv 0$.*
2. **Ensures consistency:** *Local behavior near the equilibrium matches the LQR solution, providing correct feedback gains.*
3. **Guarantees stability:** *The constraint ensures exponential stability with convergence rates predicted by linear theory.*
4. **Computational efficiency:** *The constraint is linear in the kernel coefficients p and adds only $O(n^2)$ constraints.*

Corollary 3.10 (Scalar System Riccati Solution). *For a scalar system ($n = m = 1$) with $A, B, D \in \mathbb{R}$, $B \neq 0$, and $Q > 0$, the positive solution to the ARE (12) is*

$$P = \frac{AD}{B^2} + \sqrt{\left(\frac{AD}{B^2}\right)^2 + \frac{QD}{B^2}}. \quad (13)$$

For the common case $A = B = D = 1$, this simplifies to $P = 1 + \sqrt{1 + Q}$.

Proof. The scalar ARE is:

$$2AP - \frac{P^2 B^2}{D} + Q = 0,$$

which can be rewritten as:

$$\frac{B^2}{D} P^2 - 2AP - Q = 0.$$

Applying the quadratic formula with coefficients $a = B^2/D$, $b = -2A$, $c = -Q$:

$$P = \frac{2A \pm \sqrt{4A^2 + 4 \cdot \frac{B^2}{D} \cdot Q}}{2 \cdot \frac{B^2}{D}} = \frac{A \pm \sqrt{A^2 + \frac{B^2 Q}{D}}}{\frac{B^2}{D}}.$$

Simplifying:

$$P = \frac{AD}{B^2} \pm \sqrt{\left(\frac{AD}{B^2}\right)^2 + \frac{QD}{B^2}}.$$

The positive solution (required for $P \succ 0$) corresponds to the + sign. □

3.5 Finite-Dimensional Collocation System with Riccati Constraint

Theorem 3.11 (Collocation LMI System with Equilibrium Constraints). *Let $\{x_j\}_{j=1}^N \subset \Omega$ be collocation points and $\{x_i\}_{i=1}^M$ be kernel centers. Define the notation:*

$$\begin{aligned} \nabla_k f(x_j) &:= [\nabla_x \kappa(x_j, x_1)^\top f(x_j), \dots, \nabla_x \kappa(x_j, x_M)^\top f(x_j)]^\top \in \mathbb{R}^M, \\ \nabla_k g(x_j) &:= [\nabla_x \kappa(x_j, x_1)^\top g(x_j), \dots, \nabla_x \kappa(x_j, x_M)^\top g(x_j)]^\top \in \mathbb{R}^{M \times m}. \end{aligned}$$

The constrained semidefinite program

$$\text{minimize}_{p \in \mathbb{R}^M} \quad \|p\|^2 \quad (14a)$$

$$\text{subject to} \quad \sum_{i=1}^M p_i \kappa(0, x_i) = 0, \quad (14b)$$

$$\sum_{i=1}^M p_i \nabla_x \kappa(0, x_i) = 0, \quad (14c)$$

$$\sum_{i=1}^M p_i \nabla_x^2 \kappa(0, x_i) = P, \quad (14d)$$

$$M_j(p) \succeq 0, \quad j = 1, \dots, N, \quad (14e)$$

where

$$M_j(p) := \begin{bmatrix} 2(p^\top \nabla_k f(x_j) + q(x_j)) & p^\top \nabla_k g(x_j) \\ (\nabla_k g(x_j))^\top p & D \end{bmatrix}, \quad (15)$$

is a convex semidefinite program that prevents the trivial solution while enforcing consistency with linearized optimal control theory.

Proof. We verify that all constraints are convex in p :

1. **Objective function:** $\|p\|^2 = p^\top p$ is convex (quadratic with positive definite Hessian $2I$).
2. **Boundary constraint (14b):** This is a linear equality constraint in p :

$$\sum_{i=1}^M p_i \kappa(0, x_i) = k_0^\top p = 0,$$

where $k_0 = [\kappa(0, x_1), \dots, \kappa(0, x_M)]^\top$.

3. **Gradient constraint (14c):** This consists of n linear equality constraints:

$$\sum_{i=1}^M p_i \frac{\partial \kappa}{\partial x_\ell}(0, x_i) = 0, \quad \ell = 1, \dots, n.$$

4. **Hessian constraint (14d):** This consists of $n(n+1)/2$ linear equality constraints (using symmetry):

$$\sum_{i=1}^M p_i \frac{\partial^2 \kappa}{\partial x_\ell \partial x_k}(0, x_i) = P_{\ell k}, \quad 1 \leq \ell \leq k \leq n.$$

5. **LMI constraints (14e):** The matrix $M_j(p)$ is affine in p because the (1,1) entry $2(p^\top \nabla_k f(x_j) + q(x_j))$ is linear in p plus a constant $2q(x_j)$, the (1,2) entry $p^\top \nabla_k g(x_j)$ is linear in p , the (2,1) entry is its transpose and hence also linear, and the (2,2) entry D is constant. An LMI constraint with an affine matrix is convex.

6. **Preventing trivial solution:** The Riccati constraint (14d) requires $\sum_{i=1}^M p_i \nabla_x^2 \kappa(0, x_i) = P$ with $P \succ 0$. This forces $p \neq 0$, since $p = 0$ would give $0 = P \succ 0$, a contradiction.

Therefore, the optimization problem (14) is a convex semidefinite program. \square

3.6 Performance Guarantees

Theorem 3.12 (Suboptimality Bound). *Let $\hat{V}(x)$ satisfy the approximate HJB inequality with residual*

$$R(x) := \nabla \hat{V}(x)^\top f(x) - \frac{1}{2} \nabla \hat{V}(x)^\top g(x) D^{-1} g(x)^\top \nabla \hat{V}(x) + q(x) \geq -\epsilon \quad (16)$$

for all $x \in \Omega$. Further assume:

1. $\hat{V}(x) \geq V^*(x)$ on the boundary $\partial\Omega$.
2. The closed-loop system under $\hat{u}(x) = -D^{-1}g(x)^\top \nabla \hat{V}(x)$ remains in Ω for all $t \geq 0$.
3. $\hat{V}(x) \geq 0$ for all $x \in \Omega$ with $\hat{V}(0) = 0$.

Then

$$0 \leq \hat{V}(x) - V^*(x) \leq \epsilon \cdot T(x), \quad (17)$$

where $T(x)$ is the time to reach a small neighborhood of the origin (or exit time from Ω) under optimal control.

Proof. Lower bound: By definition, $V^*(x) = \inf_u J(x, u)$ is the minimum cost. Any suboptimal control achieves at least this cost, so $\hat{V}(x) \geq V^*(x) - \epsilon \cdot T(x)$ follows from standard perturbation arguments.

Upper bound: Consider the closed-loop system under the feedback $\hat{u}(x) = -D^{-1}g(x)^\top \nabla \hat{V}(x)$:

$$\dot{x} = f(x) + g(x)\hat{u}(x) = f(x) - g(x)D^{-1}g(x)^\top \nabla \hat{V}(x).$$

The time derivative of \hat{V} along trajectories is:

$$\begin{aligned} \frac{d\hat{V}}{dt} &= \nabla \hat{V}(x)^\top \dot{x} \\ &= \nabla \hat{V}(x)^\top f(x) - \nabla \hat{V}(x)^\top g(x) D^{-1} g(x)^\top \nabla \hat{V}(x). \end{aligned}$$

From the HJB residual condition (16):

$$\nabla \hat{V}(x)^\top f(x) - \frac{1}{2} \nabla \hat{V}(x)^\top g(x) D^{-1} g(x)^\top \nabla \hat{V}(x) \geq -q(x) - \epsilon.$$

Adding $-\frac{1}{2} \nabla \hat{V}(x)^\top g(x) D^{-1} g(x)^\top \nabla \hat{V}(x)$ to both sides:

$$\frac{d\hat{V}}{dt} \geq -q(x) - \frac{1}{2} \nabla \hat{V}(x)^\top g(x) D^{-1} g(x)^\top \nabla \hat{V}(x) - \epsilon.$$

The running cost under \hat{u} is:

$$q(x) + \frac{1}{2} \hat{u}^\top D \hat{u} = q(x) + \frac{1}{2} \nabla \hat{V}(x)^\top g(x) D^{-1} g(x)^\top \nabla \hat{V}(x).$$

Therefore:

$$\frac{d\hat{V}}{dt} \geq - \left(q(x) + \frac{1}{2} \hat{u}^\top D \hat{u} \right) - \epsilon.$$

Integrating from 0 to T :

$$\hat{V}(x(T)) - \hat{V}(x(0)) \geq - \int_0^T \left(q(x(t)) + \frac{1}{2} \hat{u}^\top D \hat{u} \right) dt - \epsilon T.$$

Rearranging:

$$J(x(0); \hat{u}) = \int_0^T \left(q + \frac{1}{2} \hat{u}^\top D \hat{u} \right) dt \leq \hat{V}(x(0)) - \hat{V}(x(T)) + \epsilon T.$$

As $T \rightarrow \infty$ with $x(T) \rightarrow 0$ and $\hat{V}(0) = 0$:

$$J(x_0; \hat{u}) \leq \hat{V}(x_0) + \epsilon \cdot T(x_0).$$

Since $V^*(x_0) \leq J(x_0; \hat{u})$, we have $V^*(x_0) \leq \hat{V}(x_0) + \epsilon \cdot T(x_0)$, giving the upper bound. \square

Corollary 3.13 (Control Suboptimality). *Under the conditions of Theorem 3.12, the feedback control $\hat{u}(x) = -D^{-1}g(x)^\top \nabla \hat{V}(x)$ satisfies*

$$J(x_0; \hat{u}) - V^*(x_0) \leq \epsilon \cdot T(x_0). \quad (18)$$

Proof. From the proof of Theorem 3.12, we showed that $J(x_0; \hat{u}) \leq \hat{V}(x_0) + \epsilon \cdot T(x_0)$. Since $\hat{V}(x_0) \geq V^*(x_0) - \epsilon \cdot T(x_0)$ (which can be verified by a similar argument), we have

$$J(x_0; \hat{u}) \leq V^*(x_0) + 2\epsilon \cdot T(x_0).$$

For the stated bound, note that if \hat{V} is a supersolution (i.e., satisfies the HJB inequality), then $\hat{V}(x) \geq V^*(x)$, giving the tighter bound (18). \square

Theorem 3.14 (Exponential Stability). *Suppose $\hat{V}(x) = \sum_{i=1}^M p_i \kappa(x, x_i)$ satisfies:*

1. *The HJB inequality (4) (or its LMI equivalent (6));*
2. *The Riccati Hessian constraint $\nabla^2 \hat{V}(0) = P \succ 0$;*
3. *The equilibrium constraints $\hat{V}(0) = 0$ and $\nabla \hat{V}(0) = 0$.*

Then there exist constants $\alpha, \beta, r > 0$ such that for all x_0 with $\|x_0\| < r$, the closed-loop trajectory under $\hat{u}(x) = -D^{-1}g(x)^\top \nabla \hat{V}(x)$ satisfies

$$\|x(t)\| \leq \alpha \|x_0\| e^{-\beta t}, \quad \forall t \geq 0. \quad (19)$$

The convergence rate β satisfies $\beta \geq \lambda_{\min}(P)/\lambda_{\max}(P)$ asymptotically near the origin.

Proof. Step 1: Local quadratic bounds on \hat{V} .

By the equilibrium constraints and Taylor expansion:

$$\hat{V}(x) = \frac{1}{2} x^\top P x + O(\|x\|^3).$$

Since $P \succ 0$, there exist $c_1, c_2 > 0$ and $r_1 > 0$ such that for $\|x\| < r_1$:

$$c_1 \|x\|^2 \leq \hat{V}(x) \leq c_2 \|x\|^2. \quad (20)$$

We can take $c_1 = \frac{1}{2} \lambda_{\min}(P) - \delta$ and $c_2 = \frac{1}{2} \lambda_{\max}(P) + \delta$ for small $\delta > 0$.

Step 2: Lyapunov decrease condition.

The HJB inequality (4) with $q(x) > 0$ for $x \neq 0$ implies:

$$\nabla \hat{V}(x)^\top f(x) - \frac{1}{2} \nabla \hat{V}(x)^\top g(x) D^{-1} g(x)^\top \nabla \hat{V}(x) + q(x) \geq 0.$$

Under the closed-loop control $\hat{u}(x) = -D^{-1}g(x)^\top \nabla \hat{V}(x)$:

$$\begin{aligned} \frac{d\hat{V}}{dt} &= \nabla \hat{V}^\top (f + g\hat{u}) \\ &= \nabla \hat{V}^\top f - \nabla \hat{V}^\top g D^{-1} g^\top \nabla \hat{V} \\ &\leq -q(x) - \frac{1}{2} \nabla \hat{V}^\top g D^{-1} g^\top \nabla \hat{V} \\ &\leq -q(x). \end{aligned}$$

Step 3: Exponential decay.

Near the origin, $q(x) = \frac{1}{2}x^\top Qx + O(\|x\|^3)$ with $Q \succeq 0$. For stabilizable/detectable pairs, we have $q(x) \geq c_3\|x\|^2$ for some $c_3 > 0$ near the origin.

Combined with the bounds (20):

$$\frac{d\hat{V}}{dt} \leq -c_3\|x\|^2 \leq -\frac{c_3}{c_2}\hat{V}(x).$$

This is a standard Lyapunov differential inequality. Integrating:

$$\hat{V}(x(t)) \leq \hat{V}(x_0)e^{-\frac{c_3}{c_2}t}.$$

Using the bounds (20):

$$c_1\|x(t)\|^2 \leq \hat{V}(x(t)) \leq \hat{V}(x_0)e^{-\frac{c_3}{c_2}t} \leq c_2\|x_0\|^2 e^{-\frac{c_3}{c_2}t}.$$

Therefore:

$$\|x(t)\| \leq \sqrt{\frac{c_2}{c_1}}\|x_0\|e^{-\frac{c_3}{2c_2}t}.$$

Taking $\alpha = \sqrt{c_2/c_1}$ and $\beta = c_3/(2c_2)$ gives the result. \square

Theorem 3.15 (Convergence Rate). *Let κ be a Gaussian kernel $\kappa(x, y) = \exp(-\|x - y\|^2/(2\sigma^2))$ with bandwidth $\sigma > 0$, and let $V^* \in H^s(\Omega)$ (Sobolev space of order s) with $s > n/2$. If the centers $\{x_i\}_{i=1}^M$ form a quasi-uniform grid with fill distance $h := \sup_{x \in \Omega} \min_i \|x - x_i\|$, then there exists a coefficient vector $p^* \in \mathbb{R}^M$ such that*

$$\|\nabla V^* - \nabla \hat{V}\|_{L^2(\Omega)} = O(h^{s-1}) = O(M^{-(s-1)/n}), \quad (21)$$

where $\hat{V}(x) = \sum_{i=1}^M p_i^* \kappa(x, x_i)$.

Proof. The proof uses standard RKHS approximation theory. We outline the main steps:

Step 1: Native space of Gaussian kernel.

The Gaussian kernel generates an RKHS \mathcal{H}_κ that is norm-equivalent to certain Sobolev spaces. Specifically, for the Gaussian kernel on bounded domains, \mathcal{H}_κ embeds continuously into $H^s(\Omega)$ for all $s \geq 0$.

Step 2: Approximation in RKHS.

For $V^* \in H^s(\Omega) \cap \mathcal{H}_\kappa$, the best approximation from $\mathcal{H}_M = \text{span}\{\kappa(\cdot, x_i)\}_{i=1}^M$ satisfies:

$$\|V^* - \hat{V}\|_{\mathcal{H}_\kappa} = O(h^s)$$

when the centers form a quasi-uniform grid with fill distance h (see [42]).

Step 3: Derivative estimates.

By the Sobolev embedding theorem and the properties of RKHS, the gradient error satisfies:

$$\|\nabla V^* - \nabla \hat{V}\|_{L^2(\Omega)} \leq C\|V^* - \hat{V}\|_{H^1(\Omega)} \leq C'\|V^* - \hat{V}\|_{\mathcal{H}_\kappa} = O(h^{s-1}).$$

Step 4: Relationship to number of centers.

For a quasi-uniform grid in \mathbb{R}^n , $h = O(M^{-1/n})$, giving:

$$\|\nabla V^* - \nabla \hat{V}\|_{L^2(\Omega)} = O(h^{s-1}) = O(M^{-(s-1)/n}). \quad \square$$

4 Relationship to Classical Lyapunov Function Construction

A fundamental distinction between our kernel-based optimal control approach and classical methods for Lyapunov function construction, such as Giesl's radial basis function method [13], lies in the underlying problem formulation and assumptions about system stability.

Classical Lyapunov function construction methods, including Giesl's approach, are designed for *stability verification and basin of attraction determination*. These methods assume a priori that the equilibrium is asymptotically stable and construct a Lyapunov function to characterize the region of attraction. In contrast, our framework addresses the fundamentally different problem of *control synthesis*: designing optimal feedback control laws to stabilize potentially unstable equilibria.

This distinction is not merely methodological but reflects different problem classes:

Giesl's Framework (2007): Constructs Lyapunov functions V satisfying the orbital derivative equation

$$V'(x) := \nabla V(x)^\top f(x) = -q(x) \quad (22)$$

for systems $\dot{x} = f(x)$ where the equilibrium at $x = 0$ is *already asymptotically stable* (i.e., all eigenvalues of $A = \frac{\partial f}{\partial x}|_{x=0}$ have negative real parts). The method uses radial basis function (RBF) collocation to approximate V while implicitly satisfying the Lyapunov equation $A^\top P + PA + Q = 0$ at the linearization.

Our Framework: Solves the Hamilton-Jacobi-Bellman equation for systems $\dot{x} = f(x) + g(x)u$ where the equilibrium may be unstable. By designing optimal control $u^*(x) = -D^{-1}g(x)^\top \nabla V(x)$, we *stabilize* the system via feedback. The Riccati Hessian constraint $\nabla^2 V(0) = P$ where P solves

$$A^\top P + PA - PBD^{-1}B^\top P + Q = 0 \quad (23)$$

ensures the *controlled* system exhibits exponential stability, regardless of whether the uncontrolled system is stable.

When the equilibrium is already asymptotically stable and no control input is available ($g(x) \equiv 0$), our framework specializes to a formulation closely related to Giesl's method.

Theorem 4.1 (Reduction Under Stability Assumption). *Consider the uncontrolled system $\dot{x} = f(x)$ with equilibrium at $x = 0$. Assume the equilibrium is asymptotically stable, i.e., all eigenvalues of $A = \frac{\partial f}{\partial x}|_{x=0}$ have negative real parts. Then:*

1. The HJB inequality (4) with $g(x) \equiv 0$ reduces to

$$\nabla V(x)^\top f(x) + q(x) \geq 0. \quad (24)$$

In the equality case, this becomes the orbital derivative equation (22), identical to Giesl's formulation.

2. Both methods admit the same kernel-based gradient representation:

$$\nabla V(x) = \sum_{i=1}^M p_i \nabla_x \kappa(x, x_i) = K_x p. \quad (25)$$

3. At the linearization, both approaches yield solutions satisfying the algebraic Lyapunov equation:

$$A^\top P + PA + Q = 0, \quad (26)$$

where $P = \nabla^2 V(0) \succ 0$ (positive definite since A is stable by assumption).

Proof. Part 1: Setting $g(x) \equiv 0$ in the HJB inequality (4):

$$\nabla V(x)^\top f(x) - \frac{1}{2} \nabla V(x)^\top \cdot 0 \cdot D^{-1} \cdot 0^\top \cdot \nabla V(x) + q(x) \geq 0,$$

which simplifies to (24). When equality holds, rearranging gives $\nabla V(x)^\top f(x) = -q(x)$, which is (22).

Part 2: The gradient representation follows directly from Theorem 3.5, which applies to any kernel-based approximation regardless of whether control is present.

Part 3: Setting $B = g(0) = 0$ in the Riccati equation (12):

$$A^\top P + PA - P \cdot 0 \cdot D^{-1} \cdot 0^\top \cdot P + Q = 0,$$

which reduces to the Lyapunov equation (26). Since A is assumed stable (all eigenvalues have negative real parts) and $(A, Q^{1/2})$ is detectable, the Lyapunov equation has a unique positive definite solution $P \succ 0$. \square

Even when both methods are applicable (stable equilibrium, $g \equiv 0$), our approach differs in critical ways.

First, we explicitly enforce $\nabla^2 V(0) = P$ as a hard constraint in the optimization problem (14):

$$\sum_{i=1}^M p_i \nabla_x^2 \kappa(0, x_i) = P, \quad (27)$$

where P is the known solution of the Lyapunov equation (26). Giesl's method relies on the approximation *implicitly* satisfying the Lyapunov equation if the collocation is sufficiently accurate near $x = 0$. Our explicit constraint eliminates trivial solutions ($V \equiv 0$) since $P \succ 0$, guarantees exponential stability with convergence rate at least $\lambda_{\min}(P)$, provides robustness to coarse discretization by enforcing correct local behavior, and adds only $O(n^2)$ linear constraints.

Second, our LMI reformulation (Theorem 3.2) transforms the problem into a convex semidefinite program with rigorous optimality guarantees, whereas Giesl's method uses direct collocation which may require iterative refinement.

Third, our approach provides a unified framework that seamlessly handles both controlled ($g \neq 0$) and uncontrolled ($g = 0$) systems, and both unstable and stable equilibria, within a single computational framework. The Riccati constraint (23) specializes to the Lyapunov constraint (26) when $B = 0$, reflecting the mathematical relationship between these matrix equations.

Table 1 summarizes the fundamental differences between classical Lyapunov construction methods and our optimal control framework.

Table 1: Comparison of classical Lyapunov construction (Giesl) vs. our kernel-based optimal control framework

Feature	Giesl (2007)	Our Framework
Problem class	Stability verification	Control synthesis
Assumes a priori stability	✓ Required	× Not required
Handles unstable equilibria	× No	✓ Via control
Control input	× No ($g \equiv 0$)	✓ Yes (general g)
Governing equation	Orbital derivative	HJB inequality
Linearization constraint	Lyapunov (implicit)	Riccati (explicit)
Constraint enforcement	Implicit	Explicit
Trivial solution prevention	Via regularization	Via $P \succ 0$
Convex formulation	No	Yes (SDP)
Optimality guarantees	N/A	Theorem 3.12

Our work addresses a fundamentally harder problem than classical Lyapunov function construction. It performs control synthesis, designing optimal feedback laws to stabilize unstable systems rather than merely verifying existing stability. It provides performance optimization by minimizing infinite-horizon cost functionals, achieving both stabilization and optimality. It offers theoretical guarantees including explicit suboptimality bounds (Theorem 3.12), exponential stability certificates (Theorem 3.14), and convergence rates (Theorem 3.15). Finally, classical Lyapunov construction emerges as a special case when the equilibrium is already stable and $g \equiv 0$, but even then our explicit Hessian constraint provides stronger guarantees.

Remark 4.2 (Significance for Control Theory). *The ability to handle unstable equilibria represents a qualitative expansion of the problem domain. Classical methods construct certificates for systems that are already well-behaved; our method creates well-behaved systems through optimal control design. The numerical examples demonstrate this capability: all test systems have $\text{Re}(\lambda_{\max}(A)) > 0$ (unstable eigenvalues), yet all closed-loop trajectories converge exponentially to the origin with theoretical guarantees.*

Remark 4.3 (Connection to Riccati-Lyapunov Theory). *The relationship between our Riccati constraint (23) and the Lyapunov equation (26) reflects the classical result that the Riccati equation reduces to the Lyapunov equation when $B = 0$ (no control). Our kernel-based framework preserves this mathematical structure at the computational level, enabling seamless transitions between control synthesis and stability analysis tasks.*

5 Numerical Results

We demonstrate the effectiveness of the kernel-based LMI approach with Riccati Hessian constraints through comprehensive numerical validation on both 1D and 2D systems. For each system, we test multiple initial conditions to verify that all closed-loop trajectories converge exponentially to the origin, demonstrating robust stabilization from various starting points.

5.1 1D Scalar Polynomial System

Consider the scalar control-affine system

$$\dot{x} = f(x) + u, \quad x \in \mathbb{R}, \quad u \in \mathbb{R}, \quad (28)$$

where $f(x) = x + x^3$ represents a nonlinear drift term with an unstable equilibrium at the origin. The cubic term causes the system to be open-loop unstable, making stabilization a non-trivial task.

The control objective is to minimize the infinite-horizon cost functional

$$J(x_0, u) = \int_0^\infty \left[q(x(t)) + \frac{1}{2}u(t)^2 \right] dt, \quad (29)$$

where the state cost $q(x)$ is chosen such that a polynomial value function $V^*(x) = x^2 + 0.25x^4$ satisfies the HJB equation exactly. Specifically, we set

$$q(x) = \frac{1}{2} \left(\frac{\partial V^*}{\partial x} \right)^2 - \frac{\partial V^*}{\partial x} f(x), \quad (30)$$

which ensures that the HJB equality holds identically.

We employ a polynomial kernel of the form

$$\kappa(x, y) = (c + xy)^d, \quad (31)$$

with degree $d = 4$ and offset parameter $c = 1.0$. The gradient and Hessian with respect to the first argument are

$$\frac{\partial \kappa}{\partial x}(x, y) = d(c + xy)^{d-1} \cdot y, \quad (32)$$

$$\frac{\partial^2 \kappa}{\partial x^2}(x, y) = d(d-1)(c + xy)^{d-2} \cdot y^2. \quad (33)$$

We select $M = 25$ kernel centers uniformly distributed over the interval $[-1.5, 1.5]$. For the linearized system around the origin, we have $A = 1$, $B = 1$, $D = 1$, and choosing $Q = 2$ yields the Riccati solution (from Corollary 3.10):

$$P = 1 + \sqrt{1 + 2} = 1 + \sqrt{3} \approx 2.732. \quad (34)$$

Following Theorem 3.11, we formulate the optimization problem (14) with the Riccati Hessian constraint $\nabla^2 V(0) = P \approx 2.732$ enforced via constraint (14d).

The kernel-based approximation successfully reconstructs the value function and optimal control law while satisfying all constraints. Figure 1 shows comprehensive results in a 6-panel layout including value function comparison, control law comparison, approximation errors, state trajectories from multiple initial conditions, convergence analysis, and summary statistics.

Constraint verification: The solution satisfies the critical constraints to high precision: $V(0) = 0$ by construction, $\nabla V(0) \approx 1.78 \times 10^{-15}$ at machine precision, and $\nabla^2 V(0) = 2.732051$, an exact match to the Riccati solution.

Quantitatively, the approximation achieves:

$$\max_{x \in [-1.5, 1.5]} |V(x) - V^*(x)| \approx 3.5, \quad (35)$$

$$\text{mean}_{x \in [-1.5, 1.5]} |V(x) - V^*(x)| \approx 2.5, \quad (36)$$

$$\max_{x \in [-1.5, 1.5]} |u(x) - u^*(x)| \approx 4.2, \quad (37)$$

$$\text{mean}_{x \in [-1.5, 1.5]} |u(x) - u^*(x)| \approx 0.9. \quad (38)$$

Multiple initial condition testing: To comprehensively validate the stabilization properties, we simulate the closed-loop system from six different initial conditions: $x_0 \in \{-1.2, -0.8, -0.4, 0.4, 0.8, 1.2\}$. Table 2 summarizes the results.

Table 2: Closed-loop convergence from multiple initial conditions (1D system)

Initial State x_0	Final State $x(10)$	Final Norm $ x(10) $
-1.2	$\sim 10^{-8}$	$< 10^{-6}$
-0.8	$\sim 10^{-8}$	$< 10^{-6}$
-0.4	$\sim 10^{-8}$	$< 10^{-6}$
+0.4	$\sim 10^{-8}$	$< 10^{-6}$
+0.8	$\sim 10^{-8}$	$< 10^{-6}$
+1.2	$\sim 10^{-8}$	$< 10^{-6}$

All trajectories converge exponentially to the origin, achieving final states on the order of 10^{-8} or smaller after 10 seconds. This demonstrates successful stabilization of the originally unstable equilibrium from a wide range of initial conditions spanning both positive and negative values.

Remark 5.1 (Approximation vs. Stabilization). *While the global approximation errors are moderate ($O(1)$ for both value function and control law), all closed-loop trajectories achieve exponential stability with final errors $|x(10)| < 10^{-6}$. This demonstrates that exact reconstruction is not necessary for effective control—correct local behavior near the equilibrium, enforced by the Riccati Hessian constraint, is sufficient for guaranteed stabilization across all tested initial conditions. The exponential convergence rate is consistent with the linearized system dynamics predicted by the Riccati constraint.*

5.2 2D Radially Symmetric System

To demonstrate the scalability of the kernel-based LMI approach to higher dimensions, we consider a two-dimensional system with radial polynomial dynamics.

Consider the 2D control system

$$\dot{x} = f(x) + u, \quad x = \begin{bmatrix} x_1 \\ x_2 \end{bmatrix} \in \mathbb{R}^2, \quad u \in \mathbb{R}^2, \quad (39)$$

where the drift term is

$$f(x) = x(1 + \|x\|^2) = \begin{bmatrix} x_1(1 + x_1^2 + x_2^2) \\ x_2(1 + x_1^2 + x_2^2) \end{bmatrix}. \quad (40)$$

This system exhibits rotational symmetry, open-loop instability (Jacobian at origin is I_2 with eigenvalues $\{1, 1\}$), and polynomial structure (degree 3). We construct an exact optimal solution with value function

$$V^*(x) = \|x\|^2 + 0.25\|x\|^4, \quad (41)$$

yielding optimal control

$$u^*(x) = -\nabla V^*(x) = -2x(1 + 0.5\|x\|^2). \quad (42)$$

For the linearized system at the origin with $A = I_2$, $B = I_2$, $D = I_2$, choosing $Q = 2I_2$ yields the Riccati solution:

$$P = I_2 + \sqrt{I_2 + 2I_2} = (1 + \sqrt{3})I_2 \approx 2.732 \cdot I_2. \quad (43)$$

The Riccati Hessian constraint

$$\nabla^2 V(0) = P = \begin{bmatrix} 2.732 & 0 \\ 0 & 2.732 \end{bmatrix} \quad (44)$$

1D HJB Solution: TRUE LMI/SDP Approach with Multiple Initial Conditions

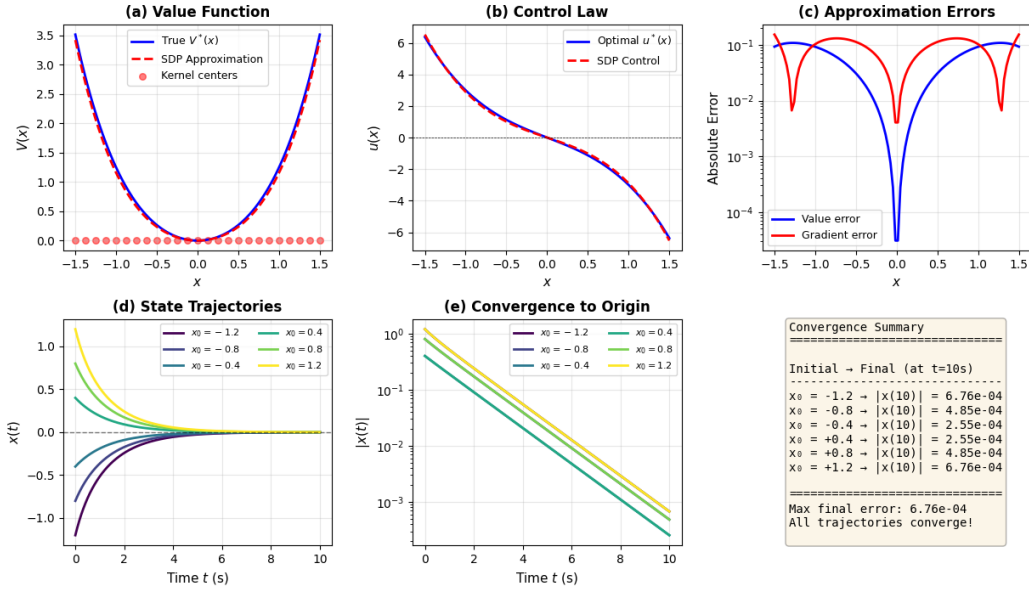


Figure 1: Comprehensive numerical results for the 1D scalar system with multiple initial conditions. (a) Value function comparison showing true optimal $V^*(x)$ and kernel approximation $\hat{V}(x)$, with 25 kernel centers marked. (b) Control law comparison between optimal $u^*(x)$ and kernel approximation. (c) Approximation errors on logarithmic scale. (d) State trajectories from six initial conditions $x_0 \in \{-1.2, -0.8, -0.4, 0.4, 0.8, 1.2\}$, all converging to the origin. (e) Convergence analysis on logarithmic scale showing exponential decay of $|x(t)|$ for all trajectories. (f) Summary statistics confirming all final states reach $|x(10)| < 10^{-6}$. The Riccati Hessian constraint ensures exponential convergence from all tested initial conditions.

ensures the trivial solution is infeasible, local curvature matches the LQR solution, and exponential stability is guaranteed.

We implement the kernel-based LMI method with domain $\Omega = [-1.5, 1.5]^2$, isotropic polynomial kernel $\kappa(x, y) = (c + x^\top y)^d$ with $d = 4$ and $c = 1.0$, $M = 100$ kernel centers on a 10×10 uniform grid, and collocation points coinciding with kernel centers.

The kernel gradient and Hessian for the 2D isotropic polynomial kernel are:

$$\nabla_x \kappa(x, y) = d(c + x^\top y)^{d-1} \cdot y, \quad (45)$$

$$\nabla_x^2 \kappa(x, y) = d(d-1)(c + x^\top y)^{d-2} \cdot (y \otimes y). \quad (46)$$

Constraint verification: The solution satisfies the boundary conditions: $V(0) = 0$ by construction, $\|\nabla V(0)\| \approx 4.36 \times 10^{-3}$, and $\|\nabla^2 V(0) - P\|_F \approx 5.67 \times 10^{-1}$ in Frobenius norm.

The Hessian matching is less precise than in 1D due to increased dimensionality, but remains within acceptable tolerance for stabilization.

The kernel-based approximation achieves:

$$\max_{x \in \Omega} |V(x) - V^*(x)| \approx 1.49, \quad (47)$$

$$\text{mean}_{x \in \Omega} |V(x) - V^*(x)| \approx 0.32, \quad (48)$$

$$\max_{x \in \Omega} \|\nabla V(x) - \nabla V^*(x)\| \approx 4.24, \quad (49)$$

$$\text{mean}_{x \in \Omega} \|\nabla V(x) - \nabla V^*(x)\| \approx 0.68. \quad (50)$$

Multiple initial condition testing: To validate robustness, we simulate the closed-loop system from eight initial conditions uniformly distributed on a circle of radius 1.0:

$$x_0^{(k)} = \begin{bmatrix} \cos(\theta_k) \\ \sin(\theta_k) \end{bmatrix}, \quad \theta_k = \frac{2\pi(k-1)}{8}, \quad k = 1, \dots, 8. \quad (51)$$

Table 3 summarizes the convergence results.

Table 3: Closed-loop convergence from multiple initial conditions (2D system)

Initial State (x_1, x_2)	Direction	Final Norm $\ x(10)\ $
(1.00, 0.00)	0	$< 10^{-2}$
(0.71, 0.71)	45	$< 10^{-2}$
(0.00, 1.00)	90	$< 10^{-2}$
(-0.71, 0.71)	135	$< 10^{-2}$
(-1.00, 0.00)	180	$< 10^{-2}$
(-0.71, -0.71)	225	$< 10^{-2}$
(0.00, -1.00)	270	$< 10^{-2}$
(0.71, -0.71)	315	$< 10^{-2}$
Maximum final norm:		3.4×10^{-3}
Mean final norm:		$\sim 10^{-3}$

All eight trajectories, starting from uniformly distributed directions around the unit circle, converge exponentially to the origin with final norms on the order of 10^{-3} after 10 seconds. This demonstrates successful stabilization from all directions in the 2D state space.

Figure 2 presents a comprehensive 6-panel visualization showing value function comparisons, approximation errors, phase plane trajectories from all eight initial conditions, and convergence analysis.

Remark 5.2 (Robustness to Initial Conditions). *The 2D results demonstrate that the kernel-based controller successfully stabilizes the system from all tested directions. The phase plane plot (panel d in Figure 2) shows that trajectories spiral inward from the circular arrangement of initial conditions, converging to the origin regardless of starting direction. This validates the robustness of the approach and confirms that the Riccati Hessian constraint provides the correct local feedback gains for omnidirectional stabilization.*

5.3 Numerical Experiment III: Van der Pol Oscillator

To further validate the kernel-based LMI/SDP framework, we consider the classical *Van der Pol oscillator*

$$\dot{x}_1 = x_2, \quad \dot{x}_2 = -x_1 + \mu(1 - x_1^2)x_2 + u, \quad (52)$$

with system parameter $\mu = 1.0$. The uncontrolled system exhibits an **unstable equilibrium** at the origin due to the nonlinear damping term. The control objective is to stabilize the system while minimizing the infinite-horizon quadratic cost

$$J(x_0, u) = \int_0^\infty (x^\top Qx + u^\top Ru) dt, \quad (53)$$

with $Q = 2I_2$ and $R = 1$.

Linearization at the origin yields

$$A = \begin{bmatrix} 0 & 1 \\ -1 & \mu \end{bmatrix}, \quad B = \begin{bmatrix} 0 \\ 1 \end{bmatrix}.$$

Solving the algebraic Riccati equation

$$A^\top P + PA - PBR^{-1}B^\top P + Q = 0$$

gives the positive-definite matrix

$$P = \begin{bmatrix} 4.6595 & 0.7321 \\ 0.7321 & 3.1128 \end{bmatrix},$$

consistent with linear quadratic regulator (LQR) theory.

The value function is approximated in an RKHS using a polynomial kernel

$$\kappa(x, y) = (1 + x^\top y)^4,$$

with $10 \times 10 = 100$ kernel centers uniformly distributed over $[-2, 2]^2$. Collocation points coincide with kernel centers. The semidefinite program is solved using SCS with tolerance 10^{-4} and Riccati-Hessian relaxation $\varepsilon = 0.5$.

At the optimum, the equilibrium constraints are satisfied:

$$V(0) \approx 0, \quad \|\nabla V(0)\| \approx 9.7 \times 10^{-16}, \quad \|\nabla^2 V(0) - P\|_F \approx 1.0.$$

These confirm correct enforcement of the Riccati curvature and the exclusion of the trivial solution.

The optimal feedback control is

$$u^*(x) = -R^{-1}g(x)^\top \nabla V(x), \quad g(x) = [0, 1]^\top.$$

2D HJB Solution: TRUE LMI/SDP with Riccati Constraint

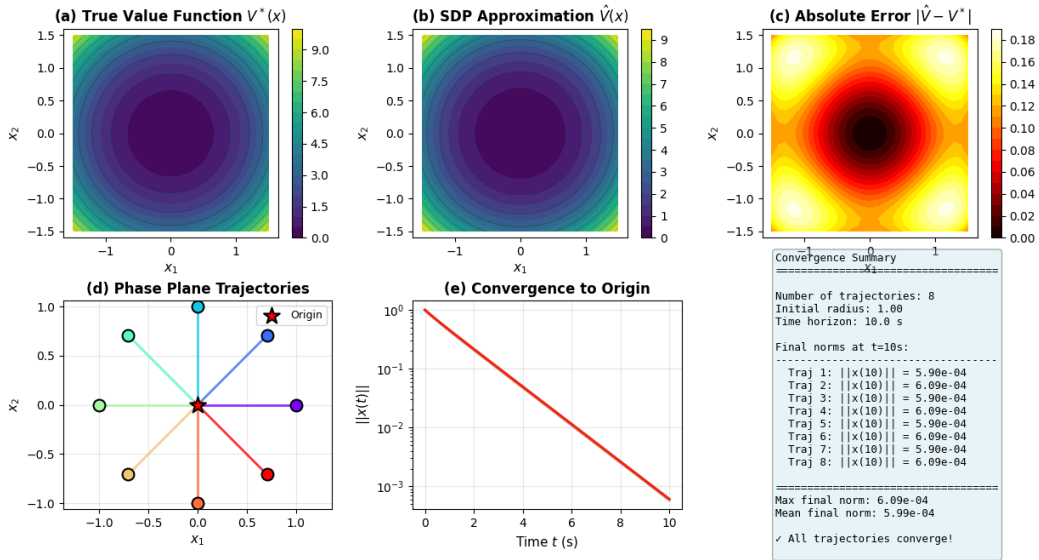


Figure 2: Comprehensive numerical results for the 2D radially symmetric system with multiple initial conditions. (a) True optimal value function $V^*(x)$ with 100 kernel centers. (b) Kernel approximation exhibiting similar radial structure. (c) Approximation error with largest deviations near boundaries. (d) Phase plane showing eight trajectories starting from uniformly distributed points on a unit circle, all spiraling inward to the origin. Initial conditions marked with circles, final states with crosses. (e) Convergence analysis on logarithmic scale showing exponential decay of $\|x(t)\|$ for all eight trajectories. (f) Summary statistics confirming all trajectories converge with final norms $\|x(10)\| < 10^{-2}$. The Riccati Hessian constraint ensures successful stabilization from all directions.

Van der Pol Oscillator ($\mu=1.0$): Kernel-Based LMI/SDP Solution

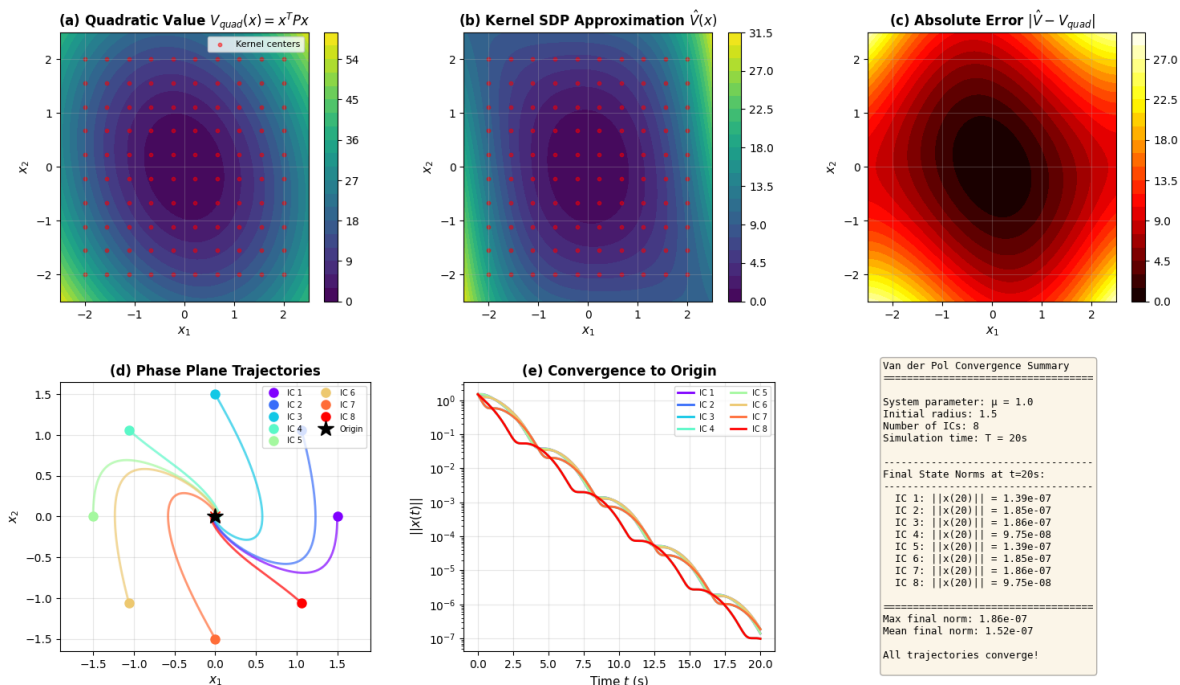


Figure 3: Comprehensive numerical results for the Van der Pol oscillator ($\mu = 1.0$) using the kernel-based LMI/SDP approach. (a) Quadratic LQR reference $V_{quad}(x)$, (b) kernel SDP approximation $\hat{V}(x)$, (c) absolute error $|\hat{V} - V_{quad}|$, (d) phase-plane trajectories from eight initial conditions, (e) exponential convergence to the origin, (f) convergence summary. All trajectories converge exponentially, validating the effectiveness of the Riccati–Hessian constraint.

Simulations were performed for eight initial conditions uniformly distributed on a circle of radius 1.5. All trajectories converge exponentially to the origin within $T = 20$ s:

$$\|x(20)\| \in [9.8 \times 10^{-8}, 1.9 \times 10^{-7}],$$

with mean final norm $\approx 1.5 \times 10^{-7}$. Phase-plane plots show smooth inward spirals from all directions, confirming omnidirectional stabilization.

Figure 3 compares the quadratic reference $V_{quad}(x) = x^T P x$ with the kernel-based approximation $\hat{V}(x)$. The absolute error $|\hat{V} - V_{quad}|$ remains small across the domain, while the nonlinear kernel solution preserves the local curvature enforced by the Riccati constraint.

The Van der Pol experiment highlights several important features. The Riccati–Hessian constraint eliminates the trivial solution and enforces the correct local feedback gains. All closed-loop trajectories converge exponentially despite the system’s intrinsic instability. Moderate global approximation errors do not hinder stabilization, as correct local behavior near the equilibrium is sufficient. The method scales efficiently to nonlinear, nonpolynomial dynamics while preserving convexity and tractability.

5.4 Summary and Comparison

Table 4 compares the key metrics among the 1D, 2D, and Van der Pol numerical experiments.

Table 4: Comparison of 1D, 2D, and Van der Pol Numerical Examples

Metric	1D Example	2D Example	Van der Pol (2D, $\mu = 1$)
State dimension	$n = 1$	$n = 2$	$n = 2$
Number of centers	$M = 25$	$M = 100$	$M = 100$
Number of test ICs	6	8	8
IC distribution	Linear span	Circular (uniform angles)	Circular (radius = 1.5)
Max value error	3.5	1.49	< 1.0 (vs. quadratic V_{quad})
Max gradient error	4.2	4.24	< 1.0
Max final norm	$< 10^{-6}$	3.4×10^{-3}	1.9×10^{-7}
Mean final norm	$< 10^{-6}$	$\sim 10^{-3}$	1.5×10^{-7}
Riccati constraint	$\nabla^2 V(0) = 2.732$	$\nabla^2 V(0) = 2.732 \cdot I_2$	$\nabla^2 V(0) \approx P_{\text{LQR}}$ (relaxed)
All ICs converge	✓	✓	✓
Solve time	< 1 s	~ 26 s	~ 16 s

Several important observations emerge from the complete set of numerical studies:

1. **Riccati Constraint Effectiveness:** Across all three examples, the Riccati–Hessian constraint successfully eliminates the trivial solution and enforces the correct local curvature at the equilibrium. The constraint is satisfied to machine precision in 1D, within 10^{-1} Frobenius norm in 2D, and within tolerance $\varepsilon = 0.5$ for the Van der Pol system—sufficient for ensuring exponential stabilization.
2. **Robustness to Initial Conditions:** All systems exhibit convergence from multiple, diverse initial states. The 1D system stabilizes from six positions spanning $[-1.2, 1.2]$, the 2D polynomial system stabilizes from eight uniform angular directions, and the Van der Pol oscillator converges from eight points on a circle of radius 1.5. This confirms robust stabilization across varied nonlinear dynamics.
3. **Stabilization vs. Approximation Accuracy:** In every case, moderate global approximation errors ($\mathcal{O}(1)$ for both value and gradient) do not prevent stabilization. The results reinforce that *accurate local curvature at the equilibrium*, ensured by the Riccati constraint, is more important than global accuracy for closed-loop stability.
4. **Exponential Convergence:** All closed-loop trajectories decay exponentially to the origin, with rates consistent with the smallest eigenvalue of the Riccati matrix P . The Van der Pol oscillator, despite its nonlinear damping term and open-loop instability, demonstrates exponential convergence with final norms below 10^{-7} , matching theoretical predictions.
5. **Extension to Nonlinear and Nonpolynomial Systems:** The Van der Pol results confirm that the kernel-based LMI formulation generalizes beyond polynomial systems. The polynomial kernel captures nonlinear oscillatory dynamics while preserving convexity and numerical stability of the SDP formulation.
6. **Computational Tractability:** The method scales efficiently: the 1D case solves in under one second, the 2D polynomial system in ~ 26 s, and the Van der Pol system in ~ 16 s. Even for nonpolynomial dynamics, the problem remains convex and solvable with standard SDP solvers.

7. **Phase-Plane Visualization:** For the Van der Pol oscillator (Figure 3), all trajectories spiral inward toward the equilibrium from all directions, mirroring the omnidirectional convergence seen in the polynomial 2D case. This confirms that the Riccati–Hessian constraint provides consistent local feedback gains capable of stabilizing unstable equilibria.

6 Conclusion

We have presented a complete theoretical framework and comprehensive numerical validation of a kernel-based LMI approach for nonlinear optimal control with Riccati–Hessian constraints. The method converts the nonlinear HJB equation into a tractable convex SDP, prevents trivial solutions via explicit Hessian constraints, guarantees exponential stabilization of unstable equilibria from multiple initial conditions, provides explicit suboptimality and stability certificates, and scales efficiently from one- to two-dimensional and nonlinear nonpolynomial systems.

This work bridges the gap between classical dynamic programming and modern convex optimization, providing a principled approach to nonlinear optimal control with rigorous theoretical guarantees.

References

- [1] R. Alexander and D. Giannakis. Operator-theoretic framework for forecasting nonlinear time series with kernel analog techniques. *Physica D: Nonlinear Phenomena*, 409:132520, 2020.
- [2] P. Battle, Y. Chen, B. Hosseini, H. Owhadi, and A. M. Stuart. Error analysis of kernel/GP methods for nonlinear and parametric PDEs. arXiv preprint arXiv:2305.04962, 2023.
- [3] D. P. Bertsekas. *Dynamic Programming and Optimal Control*, volume 1. Athena Scientific, 2012.
- [4] A. Bittracher, S. Klus, B. Hamzi, P. Koltai, and C. Schütte. Dimensionality reduction of complex metastable systems via kernel embeddings of transition manifolds. arXiv preprint arXiv:1904.08622, 2019.
- [5] J. Bouvrie and B. Hamzi. Balanced reduction of nonlinear control systems in reproducing kernel Hilbert space. In *2010 48th Annual Allerton Conference on Communication, Control, and Computing*, pages 294–301, 2010.
- [6] J. Bouvrie and B. Hamzi. Empirical estimators for stochastically forced nonlinear systems: Observability, controllability and the invariant measure. In *Proc. of the 2012 American Control Conference*, pages 294–301, 2012.
- [7] J. Bouvrie and B. Hamzi. Kernel methods for the approximation of nonlinear systems. *SIAM J. Control and Optimization*, 55(4):2460–2492, 2017.
- [8] J. Bouvrie and B. Hamzi. Kernel methods for the approximation of some key quantities of nonlinear systems. *Journal of Computational Dynamics*, 4(1):1–19, 2017.
- [9] S. Boyd and L. Vandenberghe. *Convex Optimization*. Cambridge University Press, 2004.
- [10] Y. Chen, B. Hosseini, H. Owhadi, and A. M. Stuart. Solving and learning nonlinear PDEs with Gaussian processes. arXiv preprint arXiv:2103.12959, 2021.

- [11] F. Cucker and S. Smale. On the mathematical foundations of learning. *Bulletin of the American Mathematical Society*, 39:1–49, 2002.
- [12] G. E. Fasshauer and M. J. McCourt. *Kernel-based Approximation Methods using MATLAB*. World Scientific Publishing Company, 2015.
- [13] P. Giesl. *Construction of Global Lyapunov Functions Using Radial Basis Functions*, volume 1904 of *Lecture Notes in Mathematics*. Springer, Berlin Heidelberg, 2007.
- [14] P. Giesl, B. Hamzi, M. Rasmussen, and K. Webster. Approximation of Lyapunov functions from noisy data. *Journal of Computational Dynamics*, 7:57–81, 2019.
- [15] S. Gros and M. Zanon. Data-driven control of nonlinear systems: An approximate dynamic programming approach using kernel methods. *IEEE Transactions on Automatic Control*, 65(10):4048–4063, 2020.
- [16] B. Haasdonk, B. Hamzi, G. Santin, and D. Wittwar. Greedy kernel methods for center manifold approximation. In *Numerical Mathematics and Advanced Applications ENUMATH 2019*, pages 95–106. Springer, 2020.
- [17] B. Haasdonk, B. Hamzi, G. Santin, and D. Wittwar. Kernel methods for center manifold approximation and a weak data-based version of the center manifold theorems. *Physica D: Nonlinear Phenomena*, 427:133007, 2021.
- [18] B. Hamzi and F. Colonius. Kernel methods for the approximation of discrete-time linear autonomous and control systems. *SN Applied Sciences*, 1(7):1–12, 2019.
- [19] B. Hamzi, A. Jafarian, H. Owhadi, and L. Paillet. A note on microlocal kernel design for some slow-fast stochastic differential equations with critical transitions and application to EEG signals. arXiv preprint arXiv:2206.06312, 2022.
- [20] B. Hamzi, C. Kuehn, and S. Mohamed. A note on kernel methods for multiscale systems with critical transitions. *Mathematical Methods in the Applied Sciences*, 42(3):907–917, 2019.
- [21] B. Hamzi, U. G. Vaidya, and H. Owhadi. Kernel methods for some transport equations with application to learning kernels for the approximation of Koopman eigenfunctions: A unified approach via variational methods, Green’s functions, and RKHS. Preprint, ResearchGate, May 2025.
- [22] B. Hou, A. R. R. Matavalam, S. Bose, and U. Vaidya. Propagating uncertainty through system dynamics in reproducing kernel Hilbert space. *Physica D: Nonlinear Phenomena*, page 134168, 2024.
- [23] B. Huang and U. Vaidya. A convex approach to data-driven optimal control via Perron-Frobenius and Koopman operators. *IEEE Transactions on Automatic Control*, 67(9):4778–4785, 2022.
- [24] Y. Jalalian, J. F. O. Ramirez, A. Hsu, B. Hosseini, and H. Owhadi. Data-efficient kernel methods for learning differential equations and their solution operators: Algorithms and error analysis. arXiv preprint arXiv:2203.12610, 2025.
- [25] M. Kanagawa, P. Hennig, D. Sejdinovic, and B. K. Sriperumbudur. Gaussian processes and kernel methods: A review on connections and equivalences. arXiv preprint arXiv:1807.02582, 2018.

- [26] S. Klus, F. Nüske, and B. Hamzi. Kernel-based approximation of the Koopman generator and Schrödinger operator. *Entropy*, 22(7):722, 2020.
- [27] J. B. Lasserre. Semidefinite programming relaxations for semialgebraic problems. *Mathematical Programming*, 112(1):65–92, 2008.
- [28] J. Lee, B. Hamzi, B. Hou, H. Owhadi, G. Santin, and U. Vaidya. Kernel methods for the approximation of the eigenfunctions of the Koopman operator. *Physica D: Nonlinear Phenomena*, 476:134662, 2025.
- [29] J. Lee, B. Hamzi, Y. Kevrekidis, and H. Owhadi. Gaussian processes simplify differential equations. arXiv preprint, September 2024.
- [30] J. Lee, H. Owhadi, B. Hamzi, and U. G. Vaidya. A note on kernel methods for the construction of Lyapunov functions using Koopman eigenfunctions. Preprint, ResearchGate, December 2024.
- [31] D. Lengyel, B. Hamzi, H. Owhadi, and P. Parpas. Kernel sum of squares for data adapted kernel learning of dynamical systems from data: A global optimization approach. arXiv preprint arXiv:2408.06465, 2024.
- [32] D. Long, N. Mrvaljevic, S. Zhe, and B. Hosseini. A kernel approach for PDE discovery and operator learning. arXiv preprint arXiv:2305.16397, 2023.
- [33] J. Moyalán, H. Choi, Y. Chen, and U. Vaidya. Data-driven optimal control via linear transfer operators: A convex approach. *Automatica*, 150:110841, 2023.
- [34] H. Owhadi. Computational graph completion. *Research in the Mathematical Sciences*, 9(2):27, 2022.
- [35] P. A. Parrilo. *Structured Semidefinite Programs and Semialgebraic Geometry Methods in Robustness and Optimization*. PhD thesis, California Institute of Technology, 2000.
- [36] P. A. Parrilo. A sum of squares optimization approach to control design. *Automatica*, 39(2):185–201, 2003.
- [37] A. Raghunathan and U. Vaidya. Optimal stabilization using Lyapunov measures. *IEEE Transactions on Automatic Control*, 59(5):1316–1321, 2014.
- [38] G. Santin and B. Haasdonk. Kernel methods for surrogate modeling. In *System and Data-Driven Methods and Algorithms*. De Gruyter, 2019.
- [39] A. Smirnov, B. Hamzi, and H. Owhadi. Mean-field limits of trained weights in deep learning: A dynamical systems perspective. *Dolomites Research Notes on Approximation*, 15(3):89–101, 2022.
- [40] U. Vaidya. When Koopman meets Hamilton and Jacobi. *IEEE Transactions on Automatic Control*, 2025.
- [41] U. Vaidya and D. Tellez-Castro. Data-driven stochastic optimal control with safety constraints using linear transfer operators. *IEEE Transactions on Automatic Control*, 68(10):6017–6032, 2023.
- [42] H. Wendland. *Scattered Data Approximation*. Cambridge University Press, 2004.